การจำลองการกระเจิงแบบคอมป์ตันของรังสีแกมมาในคอนกรีตเสริมเหล็กโดยใช้วิธีมอนติคาร์โล

นาย กานต์พงศ์ ชูพันธ์

วิทยานิพนธ์นี้เป็นส่วนหนึ่งของการศึกษาตามหลักสูตรปริญญาวิศวกรรมศาสตรมหาบัณฑิต
สาขาวิชานิวเคลียร์เทคโนโลยี ภาควิชานิวเคลียร์เทคโนโลยี
คณะวิศวกรรมศาสตร์ จุฬาลงกรณ์มหาวิทยาลัย
ปีการศึกษา 2543

ISBN 947-13-1019-6

SIMULATION OF GAMMA-RAY COMPTON SCATTERING IN REINFORCED CONCRETE USING THE MONTE CARLO METHOD

MR. KANPONG CHOOPHAN

A Thesis Submitted in Partial Fulfillment of the Requirements
for the Degree of Master of Engineering in Nuclear Technology
Department of Nuclear Technology
Faculty of Engineering
Chulalongkorn University
Academic Year 2000

ISBN 947-13-1019-6

Thesis Title	SIMULATION OF GAMMA-RAY SCATTERING IN REINFORCED CONCRETE USING THE MONTE CARLO METHOD
By	MR. KANPONG
Field of study	NUCLEAR TECHNOLOGY
Thesis Advisor	ASSOCIATE PROFESSOR NARES CHANKOW, M.Eng.
Thesis Co-advisor	PROFESSOR ESAM HUSSEIN, Ph.D.

Accepted by the Faculty of Engineering, Chulalongkorn University in Partial Fulfillment of the Requirements for the Master's Degree

…….…….. Dean of Faculty of Engineering
(Professor Somsak Panyakeow, Dr.Eng.)

THESIS COMMITTEE

…….. Chairman
(Associate Professor Somyot Srisatit, M.Eng)

…….. Thesis Advisor
(Associate Professor Nares Chankow, M.Eng.)

…….. Thesis Co-Advisor
(Professor Esam Hussein, Ph.D.)

…….. Member
(Sunchai Nilsuwankosit, Ph.D.)

…….. Member
(Assistant Professor Attaporn Pattarasumunt, M.Eng.)

กานต์พงศ์ ชูพันธ์ : การจำลองการกระเจิงแบบคอมป์ตันของรังสีแกมมาในคอนกรีตเสริมเหล็กโดยใช้วิธีมอนติคาร์โล (SIMULATION OF GAMMA-RAY COMPTON SCATTERING IN REINFORCED CONCRETE USING THE MONTE CARLO METHOD)
อาจารย์ที่ปรึกษา : รศ. นเรศร์ จันทน์ขาว, อาจารย์ที่ปรึกษาร่วม : Prof. Dr. Esam Hussein, 57 หน้า. ISBN 947-13-1019-6

การวิจัยนี้มีวัตถุประสงค์ที่จะศึกษาเทคนิคดิฟเฟอเรนเชียลแกมมาเรย์สแกตเทอริงสเปกโตรสโคปีในการหาขนาดและตำแหน่งของเหล็กเส้นในคอนกรีตเสริมเหล็ก โดยใช้การจำลองการเกิดการกระเจิงแบบคอมป์ตัน โดยใช้คอมพิวเตอร์โค้ด MCNP-4A การประเมินผลการจำลองทำโดยพิจารณาค่าความเปรียบต่าง ซึ่งค่าความเปรียบต่างเป็นอัตราส่วนระหว่างดิฟเฟอเรนเชียลสเปกตรัม (ความแตกต่างของสเปกตรัมการกระเจิงแบบคอมป์ตันของแท่งคอนกรีตกับของแท่งคอนกรีตเสริมเหล็ก) กับสเปกตรัมการกระเจิงแบบคอมป์ตันของแท่งคอนกรีต ในแบบการจำลองใช้แท่งคอนกรีตเสริมเหล็กขนาด 40 ซม. X 40 ซม. X 15 ซม. ซึ่งมีเหล็กขนาดเส้นผ่าศูนย์กลาง 1 ซม. ที่อยู่ลึก 3 ซม. ในการหาความสัมพันธ์ของจุดที่เกิดการกระเจิงกับตำแหน่งของหัววัดรังสีได้สมมุติว่าหัววัดรังสีเป็นแบบจุด

ได้ทดลองประยุกต์ใช้เทคนิคดิฟเฟอเรนเชียลแกมมาเรย์สแกตเทอริงสเปกโตรสโคปี ในการดูผลจากพลังงานของรังสีแกมมา ตำแหน่งของหัววัดรังสี และการตอบสนองต่อขนาดและตำแหน่งของเหล็กเส้น ผลการวิจัยพบว่า ค่าความเปรียบต่างสูงสุดเกิดขึ้นเมื่อใช้รังสีแกมมาพลังงาน 2 ล้านอิเล็กตรอนโวลต์ และมุมการกระเจิง 90 องศา สำหรับแบบจำลองนี้พบว่า ค่าความเปรียบต่างเพิ่มขึ้นตามขนาดเส้นผ่าศูนย์กลางของเหล็กเส้นและลดลงตามความลึก นอกจากนี้ยังพบว่าค่าความเปรียบต่างเพิ่มขึ้นเมื่อสอดเหล็กเส้นเข้าไปยังลำรังสีที่ตกกระทบจนถึงค่าประมาณ 0.173 ที่ระยะ 2.914 ซม. จากนั้นความเปรียบต่างเริ่มลดลงแล้วคงที่

ผลที่ได้จากการวิจัยเบื้องต้นนี้ สามารถใช้เป็นแนวทางในการออกแบบเครื่องต้นแบบและทำนายสมรรถนะของเครื่องต้นแบบ

ภาควิชา นิวเคลียร์เทคโนโลยี ลายมือชื่อนิสิต.....
สาขาวิชา นิวเคลียร์เทคโนโลยี ลายมือชื่ออาจารย์ที่ปรึกษา.....
ปีการศึกษา 2543 ลายมือชื่ออาจารย์ที่ปรึกษาร่วม.....

4170219921 : MAJOR NUCLEAR TECHNOLOGY
KEYWORD: DIFFERENTIAL GAMMA-RAY SCATTERING SPECTROSCOPY / REINFORCED CONCRETE / THE MONTE CARLO MEHOD / MCNP-4A COMPUTER CODE

KANPONG CHOOPHAN : SIMULATION OF GAMMA-RAY COMPTON SCATTERING IN REINFORCED CONCRETE USING THE MONTE CARLO METHOD. THESIS ADVISOR : ASSSOCIATE PROFESSOR NARES CHANKOW, THESIS CO-ADVISOR : PROF. ESAM HUSSEIN, Ph.D., 57 pp. ISBN 947-13-1019-6

The objective of this research was to study the differential gamma-ray scattering spectroscopy technique (DGSS) for detecting the size and location of a steel reinforcing bar in reinforced concrete by Compton scattering simulation using the MCNP-4A computer code. The contrast of the technique was examined to evaluate the results of the simulation. The contrast is defined as the ratio of differential spectrum, (the difference of the scattering spectrum of a concrete block and the scattering spectrum of reinforced concrete), to the scattering spectrum of the concrete block. In the simulation model, reinforced concrete with a dimension of 40cm x 40cm x 15cm, and 1cm-diameter of steel bar at the depth of 3 cm, was considered. To relate the scattering point to the detector location, the detector was assumed to be confined to a point.

The DGSS technique was applied to evaluate the effect of the gamma-ray source energy, the detector position and the response for size and location of the reinforcing bar. It was found that 2 MeV gamma-ray source and 90 degree of scattering angle gave the maximum contrast value. For this particular simulation set up, it was found that contrast value increased with diameter of reinforcing bar and decreased with depth. It was also found that the contrast increased while the bar was inserted into the incident beam until it reached a value of about 0.173 at 2.914 cm insertion depth, then the contrast began to decrease and then stayed constant.

These preliminary results could be used as a guide to design a prototype and predict its performance.

Department Nuclear Technology Student's Signature……

Field of study Nuclear Technology Advisor Signature……..

Academic year 2000 Co-advisor Signature…….

Acknowledgment

I gratefully acknowledge graduate school of Chulalongkorn University for the fund to support this thesis.

I would like to thank Associate Professor Nares Chankow, my thesis advisor, Professor Dr. Esam Hussein, my thesis co-advisor, Dr. Supitcha Chanyota and Dr. Sunchai Nilsuwancosit for their useful guidance.

Last but not least, I wish to give my heartfelt and grateful thanks to my beloved parents who always place the most importance on education. I should also like to acknowledge my debt to them. Without both of them, I would never have a valuable chance to develop my academic knowledge.

Contents

Contents (Cont.)

Contents (Cont.)

Table contents

Figure contents

Figure contents (Cont.)

Page

CHAPTER 1

INTRODUCTION

1.1 Background

Reinforced concrete is a construction material made by combining concrete with steel bar. The concrete is used to resist the compression which the steel bar is for the tension. This is an important material in the constructions of walls, floors, street pavements, beam and many others infrastructure. The breaking down of such structure can cause losing of properties and life. Therefore, inspection is always required. There are two ways to test a structure, destructive testing and nondestructive testing. The destructive testing is the inspection by destroying the test sample. That means the sample can not be used again after the test. In contrast, the nondestructive testing is the test that keeps the inspected sample intact during and after the testing. It is more convenient to use in field inspection.

Nondestructive testing (NDT) with radiation has the avenge of having a high penetration depth. Radiation transmission is widely used when the source and the detector can be placed at two opposite sides of the inspected object, so that the attenuation of radiation through the object is measured. It is an effective and accurate method that is easy to handle and calculate.

Figure 1.1 Reinforced concrete

However, the transmission technique may not always be possible in every case. This is due to the surrounding space constraints and the large thickness or extended nature of the inspected object Therefore, a technique based on Compton scattering provides an alternative method.

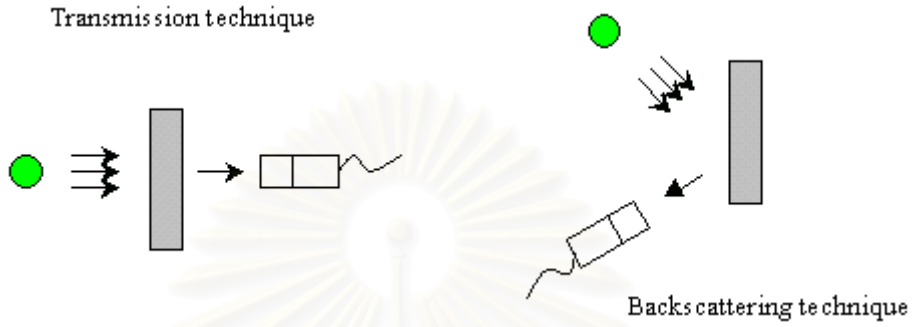

Figure 1.2 Transmission and backscattering technique

In detecting the scattering, the detector is positioned on the same side of the source so that it only measures scattered radiation from the inspected object. This method eliminates the need of accessing two opposite sides of the target object.

The disadvantage of scattering technique is its complexities. There are many parameters that must be concerned. They are such as gamma photon energy, incident angle and scattering angle etc. Therefore, it is difficult to optimize the system and to predict the results. In this case, simulation by the computer has an important role. The simulation is an experiment, which has been done on the computer by using the same conditions as they are in the nature.

MCNP-4A (Monte Carlo Neutral Particle) is a computer code widely used for solving radiation transport problems. It requires users input file that specifies geometry and the conditions in the system. The results of the simulation is contained in the output file created by the code. All interaction and statistic data of the results are also provided.

The differential gamma-ray scattering spectroscopy technique (DGSS) is applied to determine the density perturbation in a test sample. The differential spectrum, obtained by subtracting the sample spectrum (reinforced concrete) by the reference spectrum (concrete block only), contains the information characterizing the reinforcing bar in the reinforced concrete.

The main theme of this thesis is to apply the DGSS technique as an NDT technique for inspecting the reinforcing bar in the reinforced concrete.

1.2 Objective

The objective of this work is to study the differential gamma-ray scattering spectroscopy technique (DGSS) response for the size and the location of the steel reinforcing bar in the reinforced concrete using Compton scattering simulation by the MCNP-4A computer code.

Scope of thesis

1. Create the simulation model using the MCNP-4A computer code for simulating of gamma ray scattering in the reinforced concrete.
2. Develop the simulation model and appropriate response from the differential gamma-ray scattering spectroscopy technique (DGSS) technique.

1.4 Methodology

1. Conduct the literature search and review.
2. Create the simulation model using MCNP-4A computer code by varying
   - the positions of the source and the detector
   - the size and the location of the reinforcing bar
3. Apply the DGSS technique to the simulation result in order to evaluate the responses.
4. Conclude research results and write up the thesis.

1.5 Potential Application of the thesis

This thesis aims to obtain the effect of the size and the location of the reinforcing bar on the responses as obtained with the differential gamma-ray scattering spectroscopy technique (DGSS) responses. The results of which can be used as a guide to design a prototype device for the non-destructive testing using the differential gamma-ray scattering spectroscopy technique.

CHAPTER 2

COMPTON SCATTERING AND DGSS TECHNIQUE

2.1 *Introduction*

The differential gamma-ray scattering spectroscopy technique is an application of Compton scattering in nondestructive testing. This technique differs from the traditional transmission technique, such as the radiography or the computed tomography which requires observing the sample from many directions to reconstruct the actual cross-sectional density distribution. In the Compton scattering technique, the scattered photon energy distribution is measured. Since there is a relationship between the scattering energy and scattering angle, it is possible to relate the photon angular distribution to its energy distribution. The spectrum obtained from a tested sample is subtracted from one obtained from a reference sample. The resulting differential spectrum provides the information that characterizes the abnormality of the sample as compare with the reference.

2.2 Compton Scattering

Compton scattering is the elastic scattering of a photon by an electron, resulting a recoiled electron and a scattered photon in which both energy and momentum are conserved. The relation between the scattering angle and the energy of the scattered photon is expressed.

$$E(\theta) = \frac{E_0}{1 + \frac{E_0}{m_0 c^2}(1 - \cos\theta)} \quad \ldots\ldots(2.1)$$

where $E(\theta)$ is the energy of the photon scattered at an angle θ, E is the incident photon energy and m_0c^2 is the rest mass energy of electron (0.511 Mev.)

2.3 Compton Scattering NDT

Compton scattering depends on the electron density of the scattering medium, and in turn, its mass density. The intensity of the scattered radiation is also dependent on the electron density of the material in the inspection volume.

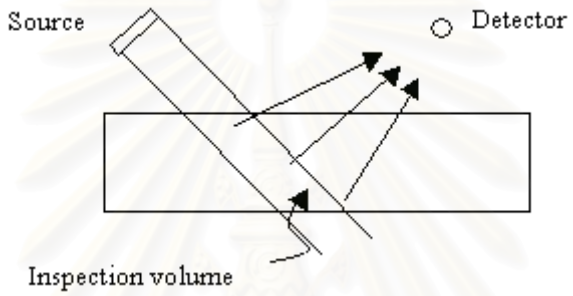

Figure 2.1 Basic geometry of Compton scattering inspection system.

The relationship between the scattering angle and the energy of scattered photon is used to determine the scattering point in the scattering medium. Information on the presence of abnormalities, location and size can then be obtained.

2.4 DGSS Technique

The energy distribution of the scattered radiation field is analyzed to obtain the information regarding the abnormalities. The basic principle of DGSS technique is to obtain the information of the differential spectrum. If the spectrum measured by the detector that views the scattered field from a sample is subtracted by one arising from a reference, then the resulting differential spectrum contains information characterizing the anomaly. It can be analyzed to obtain a density distribution by considering material properties, sample and detector geometries, and the functional relationship between the scattering angle of the gamma ray and the corresponding energy loss.

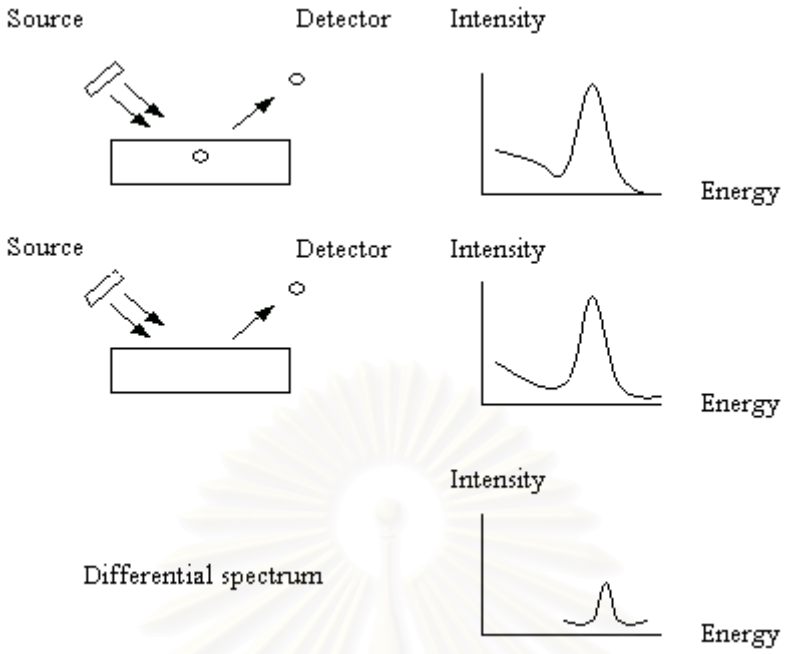

Figure 2.2 Schematic of differential spectrum.

Consider the detector in Figure 2.3. If the monoenergetic beam of gamma-ray is scattered once in the homogeneous sample of length dz along a specific beam path, the incident spectrum detected by the detector is described by the following relationship:

$$\dot{N}(\theta)d\theta = I_0 A_0 \frac{\rho N_0 Z_n}{M} \sigma(\theta)\sin\theta d\theta\delta\phi dz \qquad \ldots\ldots(2.2)$$

where $N(\theta)d\theta$ number of gamma photons scattered from the sample with angle θ into the detector,

I_0 = number of gamma photons in the collimated beam (photon/cm^2.s),

A_0 = area of beam,

Z_n = number of electron/atom in sample,

N_0 = Avogadro's number,

M = molecular weight of sample (g/mol),

ρ = density of sample (g/cm^3),

$\sigma(\theta)$ = microscopic cross section for scattering at an angle of θ per electron (cm^2),

$\delta\phi$ = azimuthal angle subtended by the detector.

As shown in Figure 2.3, the detector subtends polar angles ranging from θ_{min} to θ_{max}. The microscopic cross section $\sigma(\theta)$, which describes the polar angular distribution of the scattered photons can be calculated from Klein-Nishina formula. The azimuthal angular distribution is uniform while the energy after the scattering and the azimuthal scattering angle are independent. Since the detector measures the energy distribution of scattered photons, the single-scattered spectrum incident on the detector is determined by polar angular distribution, the relationship between polar scattering angle and scattering energy (eq. 2.1), together with the azimuthal angle intercepted by the detector.

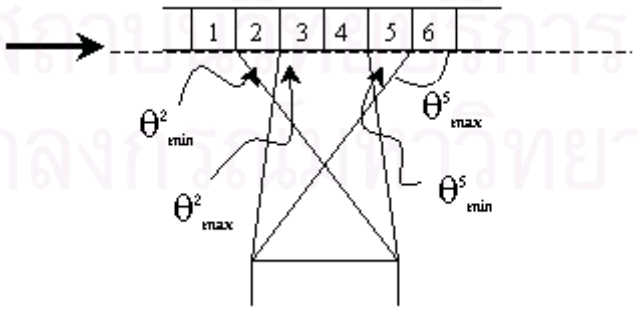

Figure 2.3 Variation of scattering angle with position of flaw along illuminated chord.

The spectrum observed by a sample at location 2 differs from that observed for location 5, since the detector intercepts different scattering angles. As the perturbation is moved from left to right in the diagram, the scattered spectrum shifts to lower energies. Thus, the shape and position of the differential spectrum contain information size and location of the abnormalities.

CHAPTER 3

MONTE CARLO CALCULATION

3.1 Introduction

Numerical experimentation, compared with physical experiments, not only is less expensive, considerably safer, and more flexible but also provides more information, better understanding of physical phenomena, and access to a wide range of experimental conditions. In addition, analysis of the results of numerical experiments can guide the selection and design of the physical experiments best suited to validating theories.

There are two ways to model nature, deterministically or stochastically. Deterministic methods involve solution of an integral or a differential equation that is cast in approximate form. The accuracy of deterministic methods is limited by how well the equations approximate the physical reality. The stochastic approach applies the Monte Carlo method and involves calculating the average or probable behavior of a system by observing the outcomes of a large number of trials. The Monte Carlo method is eminently suited to the study radiation transport, due to the complexity of the Boltzamann transport equation. The solution of the Monte Carlo method is statistically approximate, but the method provides estimates of confidence in the results.

The Monte Carlo method for radiation transport simulation had been incorporated by the Los Alamos National Laboratory in a computer code, called MCNP (Monte Carlo N-particle Transport).

3.2 Monte Carlo Method

The Monte Carlo method is a stochastic method that is used to solve the radiation transport problem by sampling a sufficient number of particles. The statistic sampling process is based on the selection of random number generated by computer. The probability distributions governing all physical events, such as scattering, absorption, or etc., are statistically sampled to describe the total phenomena. All events encountered by a particle is called “random walk”. The random walk is the result of interactions of the particle through its trajectory. The result of the random walk is that the particle does just what the physical particle does from the moment of its generation form a source until its death in some terminal category (absorption, escape or etc.). Statistical laws govern the Monte Carlo calculation as they do in nature. The probability distributions are randomly sampled using transport data to determine the outcome at each step of its life.

3.3 Random Number Generator

Digital random number generators are nowadays a standard feature in almost all computer system. The generated numbers are called pseudo random numbers as they are not pure random events. They must satisfy however two important criteria:-

- Equi-distribution : Each number has the same probability of occurrence as many other numbers in the set
- Independence : The occurrence of any given number should not depend on the previous occurrence or any subsequent occurrence of any other numbers

The modulus method is perhaps the most widely used method. Given a constant, *a*, the random number, ζ, are generated as follows:

$$\zeta_i = a\zeta_{i-1} \pmod{M} \qquad \ldots\ldots(3.1)$$

when M = 2^k and *k* is the number of bits per word in the computer being used.

3.4 Sampling Methods

There are two fundamental ways to sample probability distributions in Monte Carlo calculation:- rejection technique and direct sampling.

The sampling of particle within a volume source is one of applications of the rejection method. Suppose that the source is spherical. Three generated random numbers, ξ_1, ξ_2 and ξ_3, are calculated as follows:-

$$x = \xi_1 r \qquad y = \xi_2 r \qquad z = \xi_3 r$$

where r is the radius of spherical source. The samples of ξ_1, ξ_2 and ξ_3 are rejected if $x^2 + y^2 + z^2 = r^2$. This algorithm is called rejection technique.

A direct sampling technique may be illustrated by sampling the distance to collision. The probability of a particle travelling a distance *x* and the colliding within *dx* is

$$x = \xi_1 r \qquad y = \xi_2 r \qquad z = \xi_3 r$$

The fundamental principle for continuous probability density functions, *p(x)*, normalized so that

$$\int_0^\infty p(x)dx = 1 \qquad \ldots\ldots(3.3)$$

is that

$$\xi = P(x) = \int_0^x p(t)dt \qquad \ldots\ldots(3.4)$$

determines *x* uniquely as a function of ξ and, moreover, if ξ is uniformly distributed on $0<\xi<1$ then *x* falls with frequency *p(x)dx* in the interval (*x*, *x*+*dx*). Thus, to directly sample the distance to a collision,

$$\xi = P(x) = \int_0^x \sigma_T e^{-\sigma_T x} dx = 1 - e^{-\sigma_T x} \qquad \ldots\ldots (3.5)$$

and

$$x = -\frac{1}{\sigma_T} \ln(1-\xi) \qquad \ldots\ldots (3.6)$$

But since 1-ξ is distributed in the same manner as ξ it may be replaced by ξ.

$$x = -\frac{1}{\sigma_T} \ln(\xi) \qquad \ldots\ldots (3.7)$$

Both the rejection technique and direct sampling can be applied simultaneously for calculating complex sampling.

3.5 Estimators

Tallying is the process of scoring the parameters of interest providing the required answer. For each answer, the fractional standard deviation (fsd) or relative error is provided.

There are six standard photon estimators that are surface current estimator(F1 tally), surface flux estimator(F2 tally), track length estimator of cell flux(F4 tally), next event estimator(F5 tally) and pulse height tally(F8 Tally).

This thesis uses only the next event estimator discussing below.

3.6 Next event estimator

Next event estimator or a point detector, which is the most complicated estimator, is a deterministic estimate of the flux at a point in space.

The probability of having a random walk of the Monte Carlo particles exactly to a point is almost zero. Even if the point is finite in size, it may take billions of statistical trial, or histories, to randomly find a way to there.

The next event estimator does not require a random walk particle to reach the point. Instead, this is done by tracing a pseudo-particle without altering the original random walk path. The estimate of the flux at the point for the next event is

$$\Phi = \frac{We^{-\sigma r x} 2p(\mu)}{4\pi R^2} \quad \text{.....(3.8)}$$

where $e^{-\sigma_T x}$ is the attenuation through all mediums between the event and the next event, $2p(\mu)$ is the probability density function for scattering towards the point where the flux is detected, with μ being the cosine of the angle between the incident particle trajectory and the direction to the point, $4\pi R^2$ is the solid angle attenuation, and *R* is the distance from the event to the point of the next event.

3.7 Estimation of errors

The Monte Carlo method is a method of approximately solving mathematical and physical problems by simulation of random quantities. The process is repeated *N* times, each trial being independent of the others. The results of all trials are averaged together to provide an estimate of the quantity of interest. A requirement of the Monte Carlo method is statistic convergence. Estimation of the relative error can determine approximately how far the solution is from convergence.

The Monte Carlo method may be thought of as the solution to an integral

$$\int f(x)dx = 1 \qquad \ldots.(3.9)$$

where $f(x)$ is the underlying probability density function for a problem normalized so that the integral is unity.

The Monte Carlo tallies estimate the statistical “mean” value of the underlying problem probability distribution function

$$M_1 = \int xf(x)dx \qquad \ldots(3.10)$$

where M_1 is the first moment of the underlying probability distribution function and is also the “expected value”. In the Monte Carlo simulation, the expected value, or tally mean, is estimated as the average value scores, x_i, averaged all *N* histories of the Monte Carlo calculation.

$$\bar{x} = \frac{1}{N}\sum x_i \qquad \ldots.(3.11)$$

To estimate errors, the second central moment defines the variance of the distribution

$$M_2 = \int x^2 f(x)dx \qquad \ldots.(3.12)$$

which is estimated in the Monte Carlo calculation as

$$\bar{x}^2 = \frac{1}{N}\sum x_i^2 \qquad \ldots.(3.13)$$

According to the Central Limit Theorem of the theory of probability, the distribution of the sum of *N* independent, identically random variables with finite means and variance approaches a normal distribution as *N* takes on large values.

$$\lim_{N\to\infty} P\left(M_1 - as \le \bar{x} \le M_1 + as\right) = \frac{1}{2\pi}\int_a^b e^{-\frac{\bar{x}^2}{2}} dx \qquad \ldots\ldots(3.14)$$

That is, the probability that the estimates mean, $\bar{x}$, as $N \to \infty$, is between $M_1 - as$ and $M_1 + as$ can be calculated from a normal distribution.

The variance is given by

$$\sigma^2 = \int_{-\infty}^{\infty} (x - M_1)^2 f(x) dx \qquad \ldots\ldots(3.15)$$

$$= \int_{-\infty}^{\infty} x^2 f(x) dx - 2M_1 \int_{-\infty}^{\infty} x f(x) dx + M_1^2 \int_{-\infty}^{\infty} f(x) dx \quad = M_2 - M_1^2 \ldots\ldots(3.16)$$

The Monte Carlo method estimate of the sample variance is then

$$S^2 = \overline{x^2} - \bar{x}^2 \qquad \ldots\ldots(3.17)$$

The sample variance is not directly an estimate of the distribution variance. However, it can be stated that

$$\sigma^2 = \frac{N}{N-1} E\left(S^2\right) \qquad \ldots(3.18)$$

The confidence interval in the estimated value of $\bar{x}$ can be defined by $\bar{x} \pm \sigma_e$ where

$$\sigma_e = \frac{\sigma}{\sqrt{N}} \qquad \ldots\ldots(3.19)$$

Since σ is not known, the following estimate is used

$$\sigma_e^2 = \frac{\sigma^2}{N} = \frac{1}{N-1}\left[\overline{x^2} - \bar{x}^2\right] \qquad \ldots\ldots(3.20)$$

A useful quantity used in Monte Carlo calculations is called the fraction standard deviation, fsd, defined as

$$fsd. = \frac{\sigma_e}{\bar{x}} \qquad \ldots(3.21)$$

The Monte Carlo calculations usually require less than 0.05 or 5% of the fraction standard deviation value.

CHAPTER 4

SIMULATION PROCEDURE

4.1 Introduction

The simulation of Gamma-Ray scattering for inspection reinforcing bar in reinforced concrete has been study by using the MCNP-4A computer code. In this code, conditions and geometry of detection system are defined as they are in nature of the physics problem. This thesis begins with the studying of Gamma-Ray source energy by observing the response of the differential Gamma-Ray scattering spectroscopy technique, DGSS. From this technique, the contrast value is calculated. This value represenns how much the reinforcing bar is inspected. Then the locations of the detector are examined to find out the appropriate position for the detector. At last, size and locations of reinforcing bar are examined to obtain the responses from the DGSS technique.

4.2 Inspection system

4.2.1 Gamma-Ray source

The Gamma-Ray source is assigned to be a monodirectional beam disk source. The diameter is 2 cm and assumes that it has no thickness.

Figure 4.1 Gamma-Ray source

4.2.2 Detector

The measurement of the scattered spectrum is crucial to all subsequent computation analyses. For meaningful results, the detector is collimated to a point to relate point to point directly from the scattering point and the detector position.

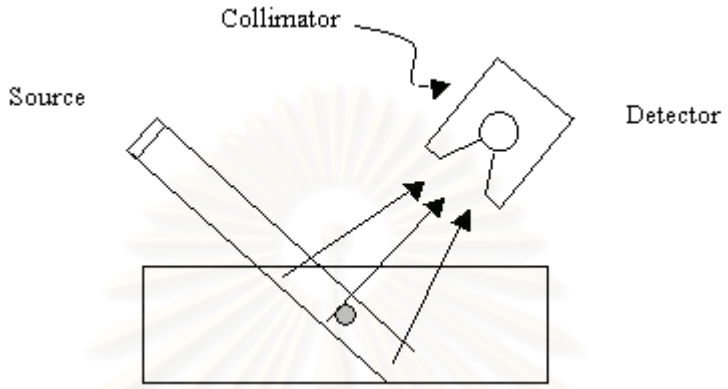

Figure 4.2 Confined wide-angle Compton-scatter inspection system

4.2.3 Reinforced concrete

Reinforced concrete is the combination of concrete block and steel bar. The concrete block is designed with a dimension of 40 x 40 x 15 cm as show in figure 4.3. The concrete is the mixture of Hydrogen 1 %, Oxygen 52.9 %, Carbon 0.1 %, Sodium 1.6 %, Manganese 0.2 %, Aluminum 3.4 %, Silicon 33.7 %, Potassium 1.3 %, Iron 1.4 % and Calcium 4.4 % by mass. And its density is 2.35 g/cm^3. The reinforcing bar or steel bar has density 7.6 g/cm^3. It is assigned as a 1 cm diameter cylinder and 50 cm long.

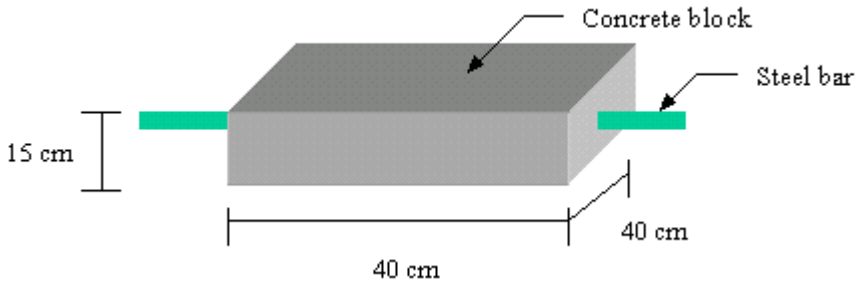

Figure 4.3 Reinforced concrete and its dimensions

4.3 Input file for the MCNP-4A computer code

An input file has the following form as shown in figure 4.4.

An input file of the MCNP-4A computer code is text file. All input files are limit to 80 columns. Alphabetic characters can be upper, lower or mixed case. A $ (dollar sign) terminates data entry. Anything that follow the $ is interpreted as a comment. Blank lines are used as delimiters and as optional terminators. Data entries are separated by one or more blanks. The first card in the file after the optional message block is the problem title card.

4.3.1 Comment Cards

Comment cards can used anywhere in the input file after the problem title card. They can used to describe the details of the problem.

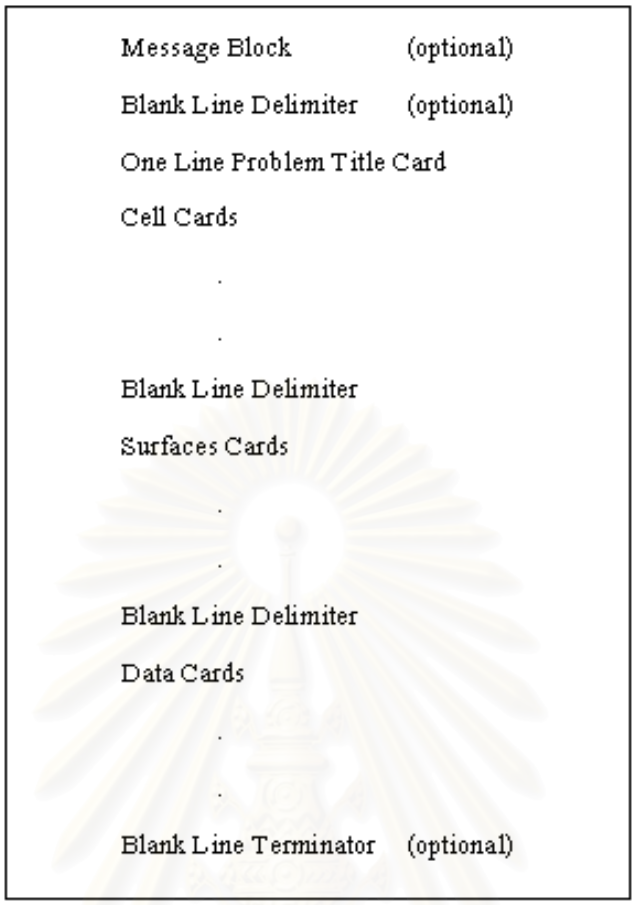

Figure 4.4 Configuration of input file of the MCNPP-4A computer code

4.3.2 Cell Cards

This computer code requires user created cells, formed by intersecting surfaces. A volume subtended by surfaces is called cell. The regions of the cells are combined with the Boolean intersection and union operation of the surfaces. A space indicates an intersection and a colon indicates a union. For example,

1 -2.35 1 -2 -3 imp:p=1

The first number is cell number and must begin in the first five columns. The next entry is the cell material number, which is arbitrarily assigned by the user. Next is the cell material density. A positive entry is interpreted as atom density in units of 10^{24} atom/cm^3. A negative entry is interpreted as mass density in units of g/cm^3. No density is entered for a void cell. The imp: p=1 is used to specify relative cell importance in the sample problem. In this example, photon only problem is specified.

4.3.3 Surface Cards

All surfaces in the MCNP-4A input file are defined by Mathematics equations. For example,

1 px 20

means that surface number 1 perpendicular to x-axis at x=20. The left side of this surface defined by x < 20 is negative sense. On the other hand, the right side of this surface defined by x > 20 is positive sense.

4.3.4 Source Definition Card

The source definition card (SDEF) is used to define source parameters and random sampling of the source. For example,

```
sdef    pos=-20 20 0  dir=1  rad=d1  vec=1 -1 0  axs=1 -1 0
        cel=3  ara=3.1415926535898E+00  erg=0.662  sur=7
si1     1.0    $ source information card (radius of source)
sp1     -21 1    $ source probability card
```

The source center is located at coordinate (-20, 20, 0) on surface 7 in cell 3, with an energy of 0.662 MeV. The source has diameter 2 cm(defined by si1 1.0) perpendicular to AXS = 1 –1 0. The area of the source surface is 3.1415926535898. The direction of beam is along the VEC = 1 –1 0 that defined by DIR=1. And the probability of source sampling is biased by a power law, $p(x) = c|x|^{1}$, defined by sp1 -21 1.

4.3.5 Mode Card

In this thesis, the photon-only mode is used to eliminate the unnecessary calculation of electron transport. Although primary photons can induce secondary photons, the occurred photons have low energy and are out of range of interest.

```
mode  p      $  photon-only problem
```

4.3.6 Physics Card

The physics calculation is determined by

```
Phys:p  0.662 1 1      $  no electron production, no coherent
```

Photon, with maximum energy 0.662 MeV, does not produce electron and the Coherent scattering is ignored.

4.3.7 Material Card

All data of any material used in this model is defined as follow:

```
m1        1001  -1.00E-02      8016 -5.29E-01      6012  -1.00E-03
         11023  -1.60E-02      12000 -2.00E-03       13027  -3.40E-02
         14000  -3.37E-01      19000 -1.30E-02       20000  -4.40E-02
         26000  -1.40E-02
m2        26000     1
```

The first material defined by m1 is concrete. It consists of Hydrogen 1 %, Oxygen 52.9 %, Carbon 0.1 %, Sodium 1.6 %, Manganese 0.2 %, Aluminum 3.4 %, Silicon 33.7 %, Potassium 1.3 %, Calcium 4.4 % and Iron 1.4 % by mass. The second material is of reinforcing bar that all made of steel.

4.3.8 Tally Card

```
fc5       point detector
f5:p      6.0 20.0 0 0
e5        0.1 3i 0.208 30i 0.331 3i 0.7
```

This command is used for point detector calculating any photon that goes to a coordinate (6, 20, 0). The last number, 0, is radius from the position of the detector. This value indicates that there is no calculation of any particle travelling into the region. Command “e5” is applied to determine energy range of the detector. The energy bins are shown as follow:

1.00000E-03 to 1.00000E-01 MeV
1.00000E-01 to 1.27000E-01 MeV
1.27000E-01 to 1.54000E-01 MeV
1.54000E-01 to 1.81000E-01 MeV
1.81000E-01 to 2.08000E-01 MeV
2.08000E-01 to 2.11968E-01 MeV
2.11968E-01 to 2.15935E-01 MeV
2.15935E-01 to 2.19903E-01 MeV
2.19903E-01 to 2.23871E-01 MeV
2.23871E-01 to 2.27839E-01 MeV
2.27839E-01 to 2.31806E-01 MeV
2.31806E-01 to 2.35774E-01 MeV
2.35774E-01 to 2.39742E-01 MeV
2.39742E-01 to 2.43710E-01 MeV
2.43710E-01 to 2.47677E-01 MeV
2.47677E-01 to 2.51645E-01 MeV
2.51645E-01 to 2.55613E-01 MeV
2.55613E-01 to 2.59581E-01 MeV
2.59581E-01 to 2.63548E-01 MeV
2.63548E-01 to 2.67516E-01 MeV
2.67516E-01 to 2.71484E-01 MeV
2.71484E-01 to 2.75452E-01 MeV
2.75452E-01 to 2.79419E-01 MeV
2.79419E-01 to 2.83387E-01 MeV
2.83387E-01 to 2.87355E-01 MeV
2.87355E-01 to 2.91323E-01 MeV

2.91323E-01 to 2.95290E-01 MeV

2.95290E-01 to 2.99258E-01 MeV

2.99258E-01 to 3.03226E-01 MeV

3.03226E-01 to 3.07194E-01 MeV

3.07194E-01 to 3.11161E-01 MeV

3.11161E-01 to 3.15129E-01 MeV

3.15129E-01 to 3.19097E-01 MeV

3.19097E-01 to 3.23065E-01 MeV

3.23065E-01 to 3.27032E-01 MeV

3.27032E-01 to 3.31000E-01 MeV

3.31000E-01 to 4.23250E-01 MeV

4.23250E-01 to 5.15500E-01 MeV

5.15500E-01 to 6.07750E-01 MeV

6.07750E-01 to 7.00000E-01 MeV

The energy range of interest is from 0.208 to 0.331 MeV. These values are energy of once scattered photons from top and bottom of the concrete block.

4.3.9 Termination Command

nps 300000

The MCNP-4A computer code calculation will terminate when 300,000 particles are sampled which the relative error or fraction standard deviation of the results less than 0.05.

4.4 Contrast Value and Error Calculation

In order to obtain the contrast value of the DGSS technique two simulation models are created. First is the reinforced concrete model. Another is concrete block model that is pure concrete. Both simulation models had the same conditions and parameters, except for the reinforcing bar.

4.4.1 Contrast Value

In this thesis, contrast value is used to define the quality of reinforcing bar inspection. It is the ratio of quantity scattered photon from steel bar to the quantity of photon scattered from reinforced concrete. The quantity of scattered photon from steel bar receives from subtracting the scattered photon reinforced concrete by the scattered photon from concrete block. The contrast can be calculated from equation 4-1.

$$Contrast = \frac{C_{steel} - C_{concrete}}{C_{concrete}} \quad \ldots\ldots (4.1)$$

where C_{steel} is quantity of the scattered photon from reinforced concrete

$C_{concrete}$ is quantity of the scattered photon from concrete block

4.4.2 Error Propagation

If x, y, z,... are directly calculated from the Monte Carlo method which $\sigma_x, \sigma_y, \sigma_z, \ldots$ are known, the standard deviation for any quantity derived from these can be calculated from equation (4-2).

$$\sigma_u^2 = \left(\frac{\partial u}{\partial x}\right)^2 \sigma_x^2 + \left(\frac{\partial u}{\partial y}\right)^2 \sigma_y^2 + \left(\frac{\partial u}{\partial z}\right)^2 \sigma_z^2 + \ldots \quad \ldots\ldots (4.2)$$

where $u = u(x, y, z, ...)$ represents the derived quantity. This equation is generally known as " Error Propagation Formula ".

4.4.2.1 Sums or Differences of Data

$$u = x + y \qquad u = x - y$$

The standard deviation of $u, (\sigma_u)$ is $\sigma_u = \sqrt{\sigma_x^2 + \sigma_y^2}$ .....(4.3)

4.4.2.2 Multiplication or Division

$$u = xy \qquad u = \frac{x}{y}$$

The standard deviation of $u, (\sigma_u)$ is $\left(\frac{\sigma_u}{u}\right)^2 = \left(\frac{\sigma_x}{x}\right)^2 + \left(\frac{\sigma_y}{y}\right)^2$ .....(4.4)

4.4.3 Error of Contrast

All results of the Monte Carlo calculation are statistical estimation data, C_{steel} and $C_{concrete}$, for which the standard deviations are known, σ_{steel} and $\sigma_{concrete}$, are known. In order to obtain contrast, the data are processed through some functional manipulations, subtraction and division, according to equation (4-1). The derived quantity, contrast, is considered with its propagated error. Then the standard deviation of contrast is obtained by equation (4.5).

$$\left(\frac{\sigma_{Concrast}}{Concrast}\right)^2 = \left(\frac{\sigma_{Steel}^2 + \sigma_{Concrete}^2}{\left(C_{Steel} - C_{Concrete}\right)^2}\right) + \left(\frac{\sigma_{Concrete}}{C_{Concrete}}\right)^2 \qquad \text{....(4.5)}$$

4.5 Simulation Model

4.5.1 Evaluation of DGSS response from energy of gamma source

This study aims to determine appropriate the energy of gamma source in inspection steel bar. Because the energy effects directly to the properties of photon, it is advantageous to estimate the energy that gives maximum contrast. The energies are examined as follow: 0.2, 0.4, 0.662, 1.0, 2.0, 5.0, 15.0 and 20.0 MeV. A 1 cm-diameter steel bar is used in reinforced concrete and placed at 3 cm-depth from surface of the concrete. The detector is located at 90 degree of scattering angle and 30 cm-distance from the cross of center of the incident beam and center of the steel bar to the detector. The inspection system of the simulation is shown in Figure 4.5.

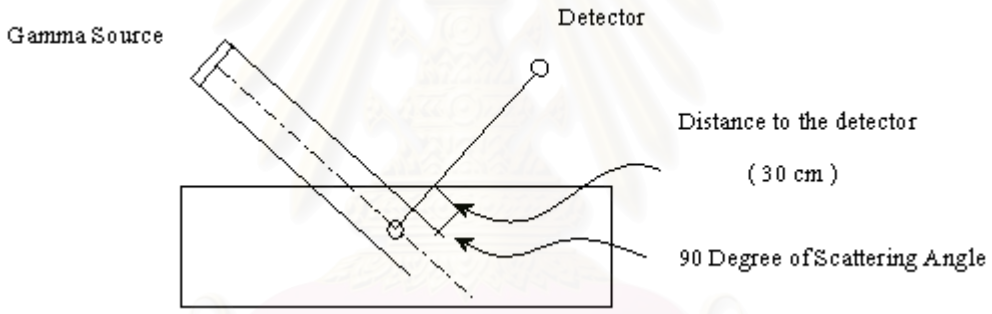

Figure 4.5 The study of gamma source energy

4.5.2 Evaluation of DGSS response from the detector arrangement

In order to study detector position, the detector is placed in many locations, 60, 65, 70, 75, 80, 85, 90, 95, 100, 105, 110, 115, 120, 125, 130, 135, 140, 145 and 150 degree of scattering angle. This angle is measured between the path of the incident photon beam and the

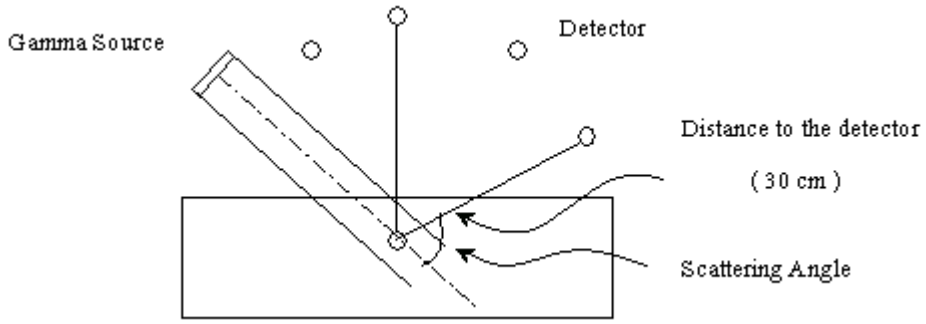

Figure 4.6 The study of detector position in any scattering angle

path of the scattered photons to the detector. The direct path length of scattered photon is 30 cm. This is in order to eliminate the effect of solid angle attenuation. This length is measured from the cross of center of the incident beam and center of the steel bar to the detector. This length is changed to 25 and 20 cm for study effect of the length to the contrast.

4.5.3 Evaluation of DGSS response of size and location of reinforcing bar

From the two simulation models above, the detection system was established. The appropriate energy of gamma source and the detector position are applied in this simulation in attempt to obtain the highest contrast value possible.

The diameter of steel is varied from 1 to 2 cm by the step of 1 mm while steel bar is fixed at 3 cm-depth form the surface of concrete. Then, the steel bar depth was changed to the 4 and 5 cm, by varying of diameter size in each step.

The last study is the insertion of steel bar gradually along its cylindrical path through the incident photon beam, as shown in figure 4.8.

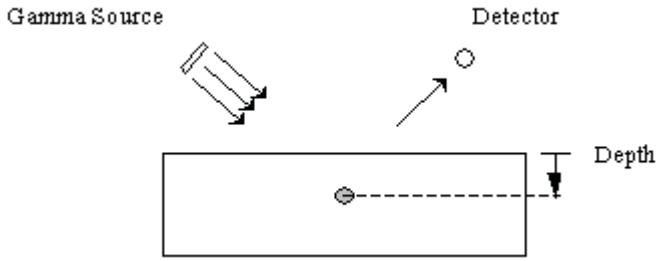

Figure 4.7 The depth of steel bar in reinforced concrete

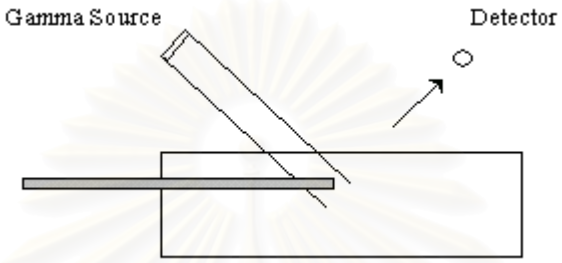

Figure 4.8 The insertion of steel bar through the incident beam

CHAPTER 5

SIMULATION RESULTS AND DISCUSSION

5.1 Introduction

This chapter provides the results of three simulations described in the last chapter together with the discussion and conclusions of the simulation results. The change of the contrast value is mainly discussed. Energy of gamma- ray source, detector positions and size and location of reinforcing bar are discussed and related to observe change of contrast value. Error of each contrast value corresponding to propagated error is also provided.

5.2 Simulation Results and Discussion

5.2.1 Evaluation of the DGSS response from energy of gamma ray source

The use of the DGSS technique is applied to evaluate the change of contrast value, as defined by equation (4.1), as a function of gamma ray energy. The results of the simulation are shown in Table 5.1, together with their propagated errors.

Table 5.1 The change of contrast value as a function of gamma ray energy with calculated standard deviation propagation

Source energy (MeV)	Contrast	Standard Deviation
0.2	0.130	0.015
0.4	0.294	0.017
0.662	0.320	0.018
0.8	0.338	0.018
1.0	0.349	0.019
2.0	0.434	0.023
5.0	0.409	0.031
10.0	0.305	0.040
15.0	0.273	0.043
20.0	0.249	0.044

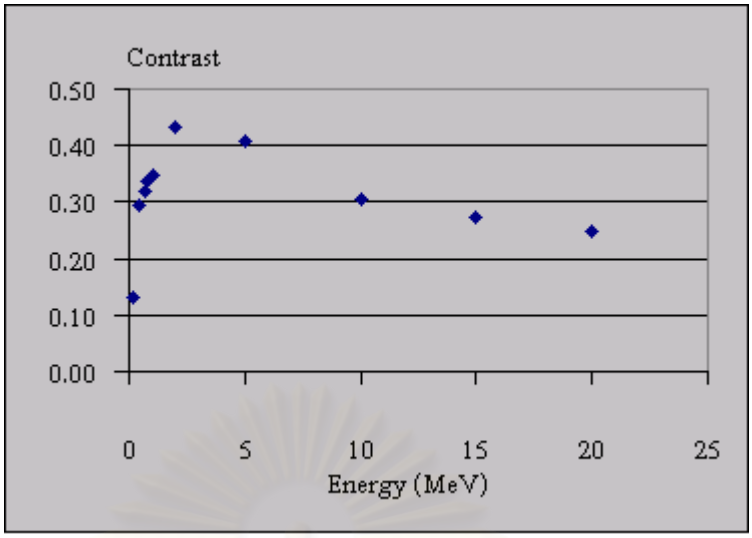

Figure 5.1 The correlation between contrast value as a function of gamma ray energy.

From the Figure 5.1, the change of contrast value tends to increase with gamma ray energy, until the value of the energy is 2 MeV, where the contrast value reaches a maximum of 0.434. Then contrast value begins to decrease. This is due to the penetration depth of photons which depends on energy of gamma ray. The higher gamma ray energy, the higher penetration depth. The change in the photon penetration can observed from the mean free-path-value, λ, shown in Table 5.2. This value indicates the maximum distance that a photon can travel in any medium before first collision. At the first period, contrast value increases with energy. It is clear that low value of gamma ray energy contributes to the low capability of photon penetration, resulting in low a contrast value. On the other hand, when energy is increased, the penetration depth of photon will increase. Then the contrast value also increases consequently.

At the second period, the contrast value begins to decrease. This is due to the Klein-Nishina theory that the probability of Compton scattering strongly increases in the forward scattering at high value of gamma ray energy.

It is clear that at the higher value of gamma ray energy, the probability of Compton scattering and consequently calculated contrast value tend to decrease with energy.

Table 5.2 The change of mean-free-path, λ, in concrete and steel as a function of gamma ray energy

Gamma ray energy (MeV)	λ (cm)	
	Steel	Concrete
0.2	0.953	3.43
0.4	0.092	4.46
0.662	0.073	5.50
0.8	0.066	6.03
1.0	0.056	6.70
2.0	0.042	9.56
5.0	0.031	14.83
10.0	0.029	18.58

5.2.2 Evaluation of DGSS response from the detector arrangement

The DGSS technique is applied to evaluate the change of contrast value as the function of detector position. The simulation results are given in Table 5.3.

Table 5.3 The change of contrast value as a function of detector position with standard deviation calculated by using error propagation. The distance from steel bar to the detector is kept at 30 cm.

Degree	Contrast	Standard Deviation
60	0.246	0.026
65	0.332	0.021
70	0.263	0.020
75	0.365	0.017
80	0.299	0.016
85	0.353	0.017
90	0.392	0.016
95	0.332	0.015
100	0.335	0.016
105	0.376	0.015
110	0.346	0.015
115	0.319	0.014
120	0.294	0.015
125	0.281	0.014
130	0.279	0.014
135	0.254	0.014
140	0.225	0.014
145	0.176	0.013
150	0.132	0.013

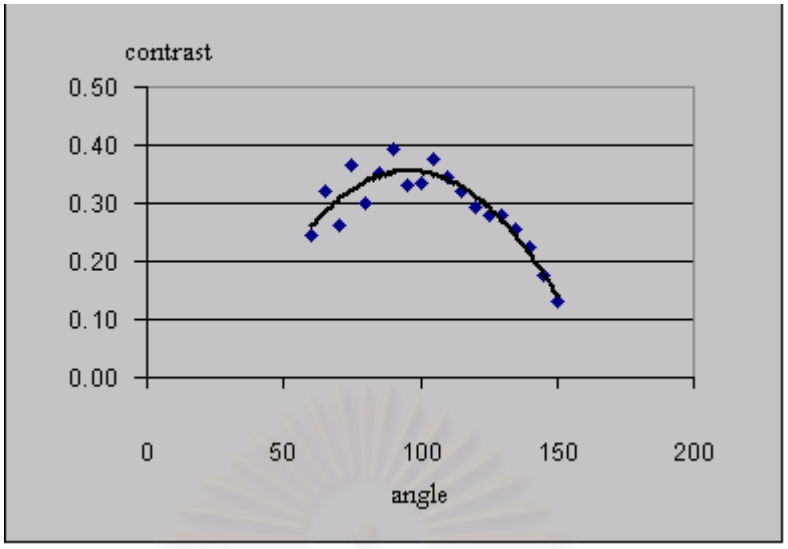

Figure 5.2 The correlation between contrast value as a function of detector position. The distance from steel bar to the detector is kept at 30 cm

From the Figure 5.2, contrast value tends to increase with the scattering angle in the first period. At the 90 degree of scattering angle, the contrast value is 0.392, which is the maximum value. Then the contrast value begins to decrease.

The change of contrast value is discussed in three parts. At the first part, the contrast value increase with the scattering angle. This is due to the path length that scattered particle travels through medium towards the detector. As shown in Figure 5.3, if the scattering angle is small, the path length is long. This path length decreases when the detector is changed to the position of higher scattering angle. So the attenuation of photons decreases. Then the contrast value increases and reaches a maximum value when the detector is positioned at the 90 degree of scattering angle.

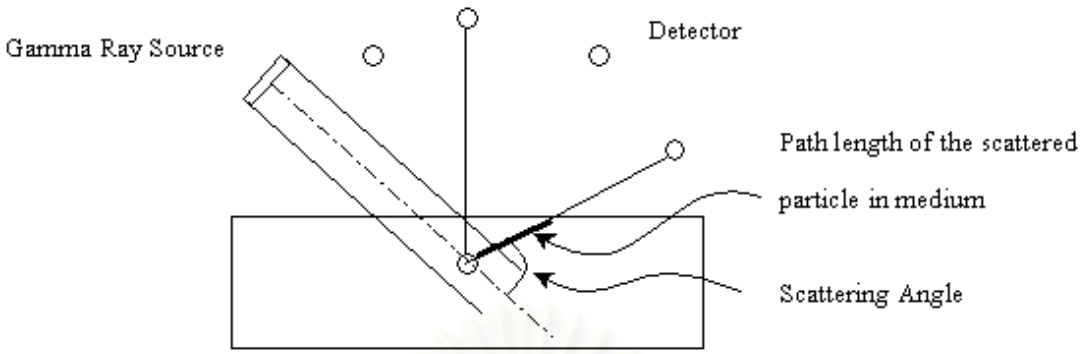

Figure 5.3 Detector position with scattering angle and path length of scattered photon travel in medium.

At the second part after 90 degree of scattering angle, the contrast value begins to decrease despite the decrement of the path length. This is due to the Klein-Nishina theory that the probability of Compton scattering decreases when the scattering angle is increased. This effect dominates over the effect of the reduction of path length after 90 degree of scattering angle.

At the last part of change of contrast value, the contrast value tends to decrease rapidly, compared with the second part. The probability of Compton scattering will decrease when the scattering angle is increased and the path length increases with the scattering angle after the detector is positioned at over 135 degree.

The distance from the steel bar to the detector was progressively changed to 25 and 20 cm. It is obviously seen that the trend in the change of the contrast value is the same as previous simulation results. But the contrast values are less than 30 cm-distance results, as shown in Figure 5.4.

Table 5.4 The change of contrast value as a function of detector position with standard deviation calculated using error propagation.
The distances from steel bar to the detector are kept at 20 and 25 cm.

cattering Angle (Degree)	20 cm.		25 cm.	
	Contrast	Standard deviation	Contrast	Standard Deviation
60	0.208	0.037	0.268	0.026
65	0.284	0.025	0.228	0.022
70	0.239	0.025	0.322	0.020
75	0.333	0.019	0.293	0.017
80	0.296	0.020	0.351	0.018
85	0.334	0.018	0.364	0.016
90	0.295	0.018	0.329	0.017
95	0.345	0.017	0.366	0.016
100	0.324	0.016	0.339	0.015
105	0.311	0.016	0.320	0.016
110	0.329	0.016	0.340	0.016
115	0.315	0.016	0.332	0.015
120	0.284	0.016	0.304	0.015
125	0.284	0.015	0.269	0.015
130	0.265	0.015	0.251	0.014
135	0.236	0.015	0.252	0.014
140	0.206	0.015	0.219	0.014
145	0.170	0.015	0.175	0.014
150	0.134	0.015	0.139	0.014

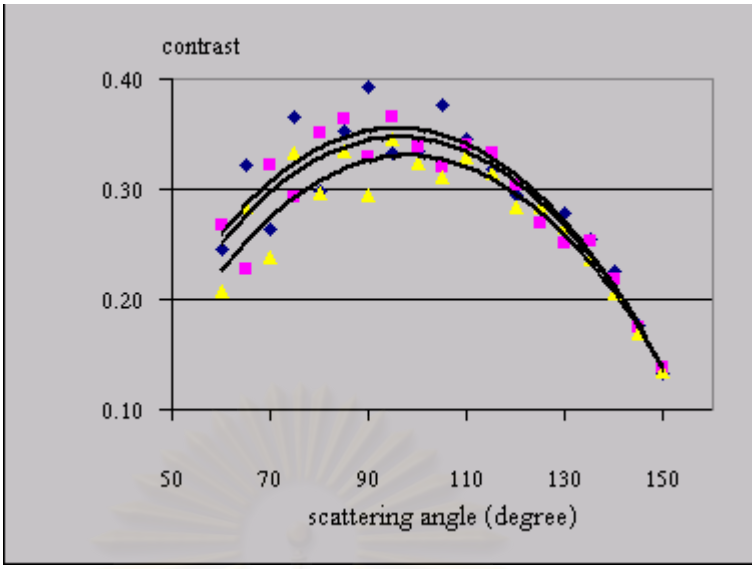

Figure 5.4 The correlation between contrast value as a function of detector position. The distances from steel bar to the detector are kept at 20, 25 and 30 cm.

♦ represents the contrast value of 30 cm distance.

□ represents the contrast value of 25 cm distance.

Δ represents the contrast value of 20 cm distance.

From the Figure 5.4, it is found that the contrast value tends to increase with the distance measured from the steel bar to the detector. This is due to the field-of-view of the detector that increases with the distance, consequently more volume of the steel bar is inspected as shown in Figure 5.5a and Figure 5.5b. Then the contrast value increases.

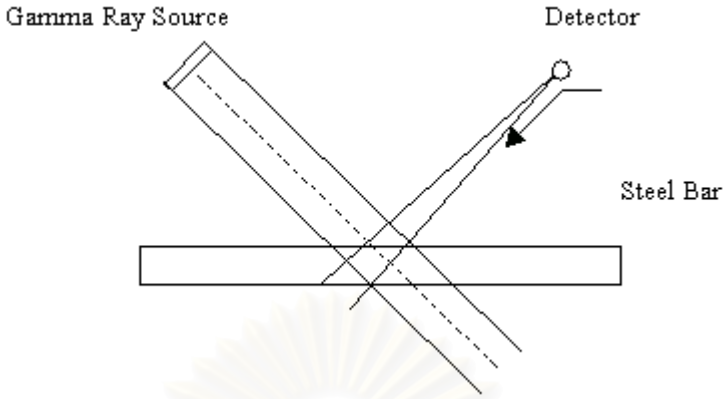

Figure 5.5a The field of view of the detector when the distance from the steel bar to the detector is 30 cm.

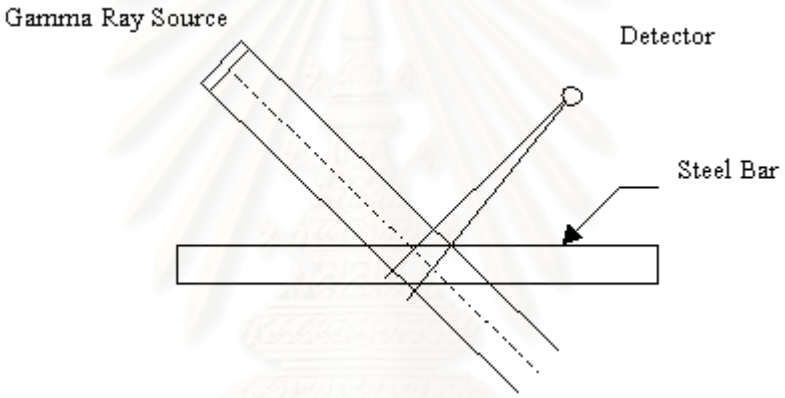

Figure 5.5b The field of view of the detector when the distance from the steel bar to the detector is 25 cm.

5.2.3 Evaluation of DGSS response of size and location of reinforcing bar

Depth and diameter of steel bar are varied to examine the response from the DGSS technique. Simulation results are shown in Table 5.5.

Table 5.5 The change of contrast value as a function of size and location of reinforcing bar with standard deviation calculated by using error propagation.

iameter (cm)	Depth 3 cm		Depth 4 cm		Depth 5 cm	
	Contrast	Standard Deviation	Contrast	Standard Deviation	Contrast	Standard Deviation
1.0	0.320	0.018	0.273	0.022	0.252	0.024
1.1	0.336	0.018	0.302	0.022	0.217	0.024
1.2	0.361	0.018	0.303	0.022	0.228	0.025
1.3	0.364	0.018	0.317	0.022	0.235	0.025
1.4	0.371	0.018	0.326	0.022	0.232	0.024
1.5	0.388	0.017	0.327	0.022	0.227	0.024
1.6	0.438	0.017	0.318	0.022	0.227	0.025
1.7	0.477	0.018	0.311	0.020	0.219	0.024
1.8	0.477	0.018	0.349	0.021	0.215	0.024
1.9	0.486	0.018	0.390	0.021	0.205	0.025
2.0	0.469	0.017	0.401	0.021	0.185	0.025

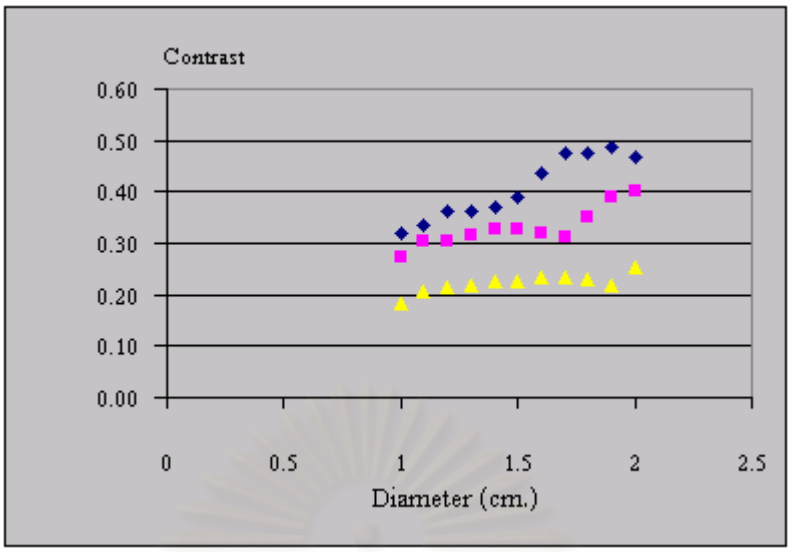

Figure 5.6 The correlation between contrast value as a function of diameter size and location of steel bar.

υ represents the contrast value at 3 cm depth.

ν represents the contrast value at 4 cm depth.

σ represents the contrast value at 5 cm depth.

From the Figure 5.6, the change of contrast tends to increase with diameter size of steel bar. For the same field-of-view of the detector, more steel is detected when the size of diameter steel is increased. Because the density of steel (7.6 g/cm^3) is higher than the density of concrete (2.35 g/cm^3), the scattering of photons from steel, which depends on the mass density of the medium, is also higher.

The change of contrast value from 3, 4 and 5 cm-depth is distributed in the same manner. But the deeper the steel bar in concrete, the lower the value of contrast. This is due to the attenuation of both incident and scattered photons in the medium.

The DGSS technique was then applied to simulate the quantity of steel bar inspected by the detector. The steel bar is inserted along its cylindrical axis through the incident photon beam as shown in Figure 4.8. The results of the simulations are shown in Table 5.6 and Figure 5.7.

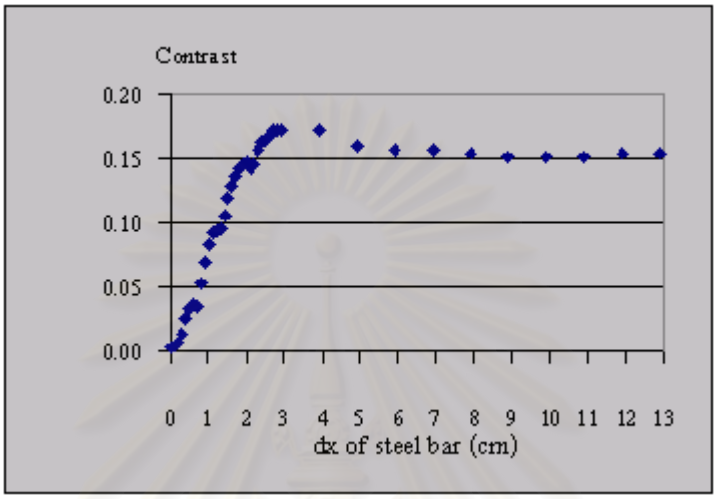

Figure 5.7 The correlation between contrast value as a function of dx of the steel bar through the incident photon beam.

As Figure 5.7 shows, the contrast value increases with increasing dx of steel rod into incident photon beam. The contrast begins to decrease when dx is 2.914 cm, where the contrast value is a maximum value. Then the contrast tends stays constant. As Shown in Figure 5.8a, the contrast value increases when the steel rod is gradually inserted into the incident photon beam.

This is due to the increase in the quantity of steel that has been inspected by field of view of the detector.

Table 5.6 The change of contrast value as a function of dx with standard deviation calculated by using error propagation.

dx (cm)	Contrast	Standard Deviation	dx (cm)	Contrast	Standard Deviation
0.014	0.003	0.017	2.014	0.147	0.016
0.114	0.004	0.025	2.114	0.142	0.017
0.214	0.008	0.016	2.214	0.145	0.018
0.314	0.013	0.015	2.314	0.158	0.018
0.414	0.026	0.015	2.414	0.163	0.018
0.514	0.034	0.014	2.514	0.165	0.018
0.614	0.036	0.014	2.614	0.168	0.018
0.714	0.036	0.015	2.714	0.172	0.018
0.814	0.053	0.015	2.814	0.172	0.018
0.914	0.069	0.016	2.914	0.173	0.018
1.014	0.083	0.015	3.914	0.172	0.018
1.114	0.093	0.016	4.914	0.161	0.018
1.214	0.094	0.015	5.914	0.157	0.018
1.314	0.095	0.016	6.914	0.157	0.018
1.414	0.106	0.053	7.914	0.155	0.018
1.514	0.119	0.016	8.914	0.152	0.018
1.614	0.129	0.016	9.914	0.152	0.018
1.714	0.137	0.016	10.914	0.152	0.018
1.814	0.142	0.016	11.914	0.154	0.018
1.914	0.145	0.017	12.914	0.154	0.018

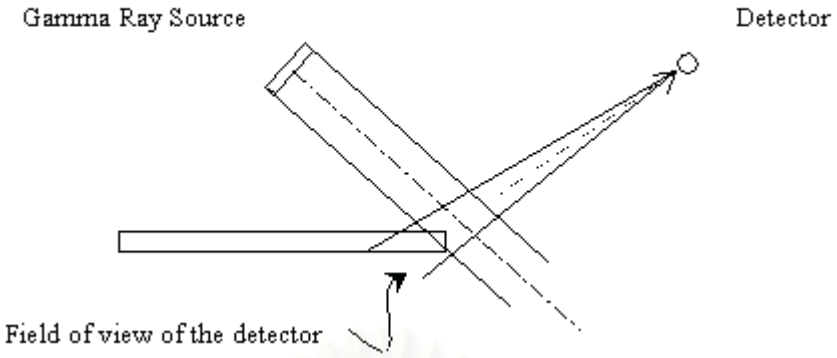

Figure 5.8a Field of view of the detector when the steel bar is initially inserted into the incident beam.

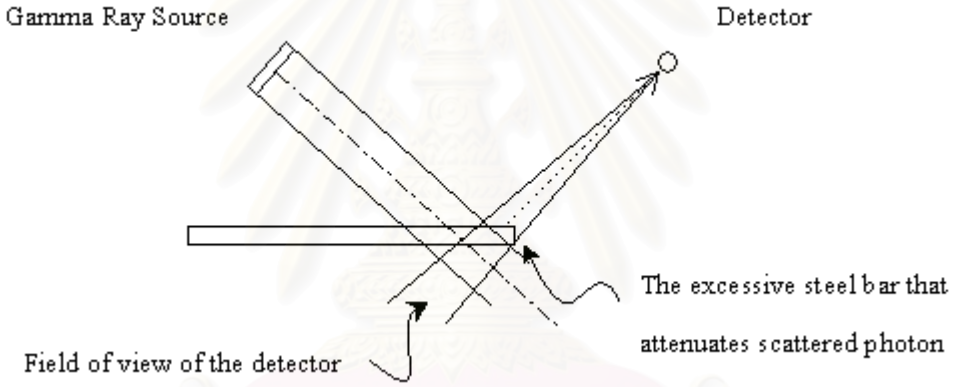

Figure 5.8b Field of view of the detector when the steel bar is inserted exceed the incident beam.

From the Figure 5.8b, it is found that the scattered photon in the field-of-view of the detector is attenuated by the excessive steel bar out of the incident photon beam. Thus, the contrast value decreases. The contrast value seems to be constant at 0.154 when steel bar is inserted through the field-of-view of the detector.

5.3 Conclusions

The performance of the DGSS technique was used to evaluate the gamma ray energy, detector position and size and location of reinforcing bar. This technique was simulated using Monte Carlo calculations to determine the optimum prototype and predict the results of any detecting system. From the optimum geometry, gamma-ray energy and detector position, the simulation models provide information on size and location of inspected steel bar in reinforced concrete. It can be conclude that this technique may be used as a guide to create a prototype that predicted results are also obtained.

In order to inspect the 1 cm-diameter of reinforcing bar in the reinforced concrete at the depth of 3 cm, the best source energy is 2.0 MeV and the best detection angle is 90 degree

References

1. Lamarsh, John R. Introduction to Nuclear Engineering. 2nd edition. Massachusetts: Addison- Wiley, 1982.
2. Knoll, Glenn F. Radiation Detection and Measurement. 1st edition. New York: John Wiley & Sons, 1979.
3. Gadner, Robin P., and Ely, Ralph L., Jr. Radioisotope Measurement Application in Engineering. New York: Reinhold, 1967.
4. Briesmeister, Judith F. MCNP-4A General Monte Carlo N-Particle Transport Code Version 4A Manual. Oak Ridge: Radiation Shielding Information Center, 1993.
5. Hussein, Esam. Monte Carlo Particle Transport with the MCNP Code. Bangkok: Department of Nuclear Technology, Chulalongkorn University, 1997.
6. Kreyszig, Erwin. Advanced Engineering Mathematics. 7th edition. Singapore: John Wiley & Sons, 1993.
7. Glasstone, Samuel, and Sesonke Alexander. Nuclear Reactor Engineering. 4th edition. London: Chapman & Hall, 1994.
8. Krane, Kenneth S. Introduction Nuclear Physics. New York: John Wiley & Sons, 1987.
9. Walpole, Ronald., and Myers, Raymond H. Probability and Statistics for Engineers and Scientists. New York: Macmillan, 1972.
10. Anghaie, S., Humphries, L.L. and Diaz, N.J., "Material Characterization and Flaw Detection, Sizing and Location by the Differential Gamma Scattering Spectroscopy Technique," Nuclear Technology, 91(1990) : 361-387
11. Arendtsz, N.V. and Hussein, E.M.A., "Energy-Spectral Compton Scatter Imagine," IEEE Transactions on Nuclear Science, 42(1995) : 2155-2172
12. NDT & E, NDT Abstracts : NDT Using Compton Scattering, NDT & E International, 28 (1995) : 189-195
13. Ho, A.C., and Hussein, E.M.A., "Quantification of Gamma-Ray Compton-Scatter Nondestructive Testin," MscE Thesis, Mechanical Engineering, University of New Brunswick, Federicton, Canada.

14. Jama, H., “Gamma-Ray Compton Scatter Nondestructive Evaluation : Determination of Angle of Scattering from the Energy Spectrum,” MscE Thesis, Mechanical Engineering, University of New Brunswick, Federiton, Canada.

15. Prettyman, T.H., Gardiner, R.P., Russ, J.C. and Verghese, K., “A combined Transmission andScattering Tomographic Approach to Composition and Density Imagine,” Applied Radiation and Isotopes, 44(1993) : 1327-1341

16. Jama, H.A. and Hussein, E.M.A., “Design Aspects of a Gamma-Ray Energy-Spectral Compton-Scatter Nondestructive Testing Method,” Applied Radiation & Isotopes, 50 (1998) : 331-342

17. Shiro, Tuzi and Otomaru, Sato, “Locating the Position of Reinforcing Bars in Reinforced Concrete Using Backscattered Gamma Rays,” Applied Radiation & Isotopes, 41(1990) : 1013-1018

Appendix

Appendix A

Input file for the MCNP-4A Computer Code

A.1 Input file for the study of scattering angle

Source :Cs-137, Monodirection ; Reinforced concrete ; Detector Arrangement at 30 cm.

```
c          cell cards
1          1        -2.35  -1 2 -3 4 -5 6 #2   imp:p=1          $  Concrete block
2          2        -7.6    -10 -9 8   imp:p=1                  $  Reinforcing bar
3          0        #2 # 1 -11  imp:p=1                        $  Internal void
4          0        11  imp:p=0                                 $  External void

c          surface cards
1          px 20.0                                             $ Plane of concrete block
2          px -20.0                                            $ Plane of concrete block
3          py 10.0                                             $ Plane of concrete block
4          py -5.0                                             $ Plane of concrete block
5          pz 20.0                                             $ Plane of concrete block
6          pz -20.0                                            $ Plane of concrete block
7          p -20.0 20.0 0.0 -21.0 19.0 1.0 -21.0 19.0 -1.0     $ Plane of source
8           pz -25.0                                           $ End of reinforcing bar
9          pz 25.0                                             $ End of reinforcing bar
10         c/z -7.0 7.0 0.5                                    $ Reinforcing bar
11         so  50                                              $ External void

c          data cards
mode p                                                         $ Photon-only problem
phys:p  .662 1 1                                               $ No electron production, no coherent
```

```
c       monodirectional disk source
sdef    pos=-20 20 0  dir=1   rad=d1  vec=1 -1 0  axs=1 -1 0
        cel=3 ara=3.1415926535898E+00  erg=0.662  sur=7
si1     1.0                                          $ Radius of source
sp1     -21 1                                        $ Provided circle, enable uncollided
m1      1001 -1.0E-02  8016 -5.29E-01  6012 -1.0E-03
        11023 -1.6E-02  12000 -2.0E-03  13027 -3.4E-02
        14000 -3.37E-01  19000 -1.3E-02  20000 -4.4E-  $ Concrete contents
        02  26000 -1.4E-02
m2      26000 1                                      $ Steel Content
fc5     point detector
f5:p    21.97777004 14.76458909 0 0                  $ Position of the detector at 60 degree
f15:p   21.19077025 17.26062731 0 0                   $ Position of the detector at 65 degree
f25:p   20.18922067 19.67857559 0 0                  $ Position of the detector at 70 degree
f35:p   18.98074375 22.00003181 0 0                  $ Position of the detector at 75 degree
f45:p   17.57453675 24.20732819 0 0                  $ Position of the detector at 80 degree
f55:p   15.98130181 26.28366581 0 0                  $ Position of the detector at 85 degree
f65:p   14.21316448 28.2132424 0 0                   $ Position of the detector at 90 degree
f75:p   12.28358139 29.98137265 0 0                  $ Position of the detector at 95 degree
f85:p   10.20723793 31.57459995 0 0                  $ Position of the detector at 100 degree
f95:p   7.999936378 32.98079885 0 0                  $ Position of the detector at 105 degree
f105:p  5.678475723 34.18926725 0 0                  $ Position of the detector at 110 degree
f115:p  3.26052376 35.19080794 0 0                   $ Position of the detector at 115 degree
f125:p  0.764482652 35.97779856 0 0                  $ Position of the detector at 120 degree
f135:p  -1.790651134 36.5442496 0 0                  $ Position of the detector at 125 degree
f145:p  -4.385431396 36.88585001 0 0                 $ Position of the detector at 130 degree
f155:p  -7.000110196 37 0 0                          $ Position of the detector at 135 degree
f165:p  -9.614788158 36.8858308 0 0                  $ Position of the detector at 140 degree
f175:p  -12.20956591 36.54421133 0 0                 $ Position of the detector at 145 degree
f185:p  -14.76469553 35.97774151 0 0                 $ Position of the detector at 150 degree
e5      0.1 3i 0.276584672 30i 0.434256091 3i 0.662  $ Energy bin for the f5:p detector
```

```
e15     0.1 3i 0.265064561 30i 0.410928235 3i 0.662     $ Energy bin for the f15:p detector
e25     0.1 3i 0.255059146 30i 0.38876172 3i 0.662      $ Energy bin for the f25:p detector
e35     0.1 3i 0.246302417 30i 0.367862045 3i 0.662     $ Energy bin for the f35:p detector
e45     0.1 3i 0.238588545 30i 0.348284547 3i 0.662     $ Energy bin for the f45:p detector
e55     0.1 3i 0.231756632 30i 0.330046236 3i 0.662     $ Energy bin for the f55:p detector
e65     0.1 3i 0.225679591 30i 0.313135978 3i 0.662     $ Energy bin for the f65:p detector
e75     0.1 3i 0.220256013 30i 0.297522889 3i 0.662     $ Energy bin for the f75:p detector
e85     0.1 3i 0.215404202 30i 0.283163067 3i 0.662     $ Energy bin for the f85:p detector
e95     0.1 3i 0.211057758 30i 0.27000482 3i 0.662      $ Energy bin for the f95:p detector
e105    0.1 3i 0.207162275 30i 0.257992636 3i 0.662     $ Energy bin for the f105:p detector
e115    0.1 3i 0.203672462 30i 0.247070108 3i 0.662     $ Energy bin for the f115:p detector
e125    0.1 3i 0.200551904 30i 0.23718205 3i 0.662      $ Energy bin for the f125:p detector
e135    0.1 3i 0.197769084 30i 0.228275955 3i 0.662     $ Energy bin for the f135:p detector
e145    0.1 3i 0.195298001 30i 0.220302963 3i 0.662     $ Energy bin for the f145:p detector
e155    0.1 3i 0.193116859 30i 0.213218464 3i 0.662     $ Energy bin for the f155:p detector
e165    0.1 3i 0.191207387 30i 0.206982421 3i 0.662     $ Energy bin for the f165:p detector
e175    0.1 3i 0.189554311 30i 0.201559122 3i 0.662     $ Energy bin for the f175:p detector
e185    0.1 3i 0.188144931 30i 0.196918735 3i 0.662     $ Energy bin for the f185:p detector
nps     300000                                          $ The simulation will be stopped when
                                                        300,000 particles were sampling

print
```

A.2 Input file for the study of energy of gamma source

Source :2.0 MeV; Detector at 90 degree; 1.0 cm diameter and 3.0 cm depth of reinforcing bar

```
c          cell cards
1          1          -2.35  -1 2 -3 4 -5 6 #2   imp:p=1          $  Concrete block
2          2          -7.6    -10 -9 8   imp:p=1                  $  Reinforcing bar
3          0          #2 # 1 -11  imp:p=1                        $  Internal void
4          0          11  imp:p=0                                 $  External void

c          surface cards
1           px 20.0                  $ Plane of concrete block
2          px -20.0                 $ Plane of concrete block
3          py 10.0                  $ Plane of concrete block
4          py -5.0                  $ Plane of concrete block
5          pz 20.0                  $ Plane of concrete block
6          pz -20.0                 $ Plane of concrete block
7          p -20.0 20.0 0.0 -21.0 19.0 1.0 -21.0 19.0 -1.0     $ Plane of source
8          pz -25.0                 $ End of steel bar
9          pz 25.0                  $ End of steel bar
10         c/z -7.0 7.0 0.5         $ Reinforcing bar
11         so  50                   $ External void

c          data cards
mode p                              $ Photon-only problem
phys:p  2.0 1 1                     $ No electron production, no coherent
c          monodirectional disk source
sdef       pos=-20 20 0  dir=1   rad=d1  vec=1 -1 0  axs=1 -1 0
           cel=3 ara=3.1415926535898E+00  erg=0.662  sur=7
si1        1.0                      $ Radius of source
sp1        -21 1                    $ Provided circle, enable uncollided
m1         1001 -1.0E-02  8016 -5.29E-01  6012 -1.0E-03
```

```
          11023 -1.6E-02  12000 -2.0E-03  13027 -3.4E-02
          14000 -3.37E-01  19000 -1.3E-02  20000 -4.4E-     $ Concrete contents
          02  26000 -1.4E-02
m2        26000 1                $ Steel Content
fc5       point detector
f5:p      6.0 20.0 0 0           $ Position of the detector at 90 degree
e5        0.1 3i 0.2643 30i      $ Energy bin for the f5:p detector
          0.4959 3i 2.0
nps       300000       $ The simulation will be stopped when 300,000 particles were sampling
print
```

A.3 Input file for the study of diameter and depth of reinforcing bar

Source :Cs-137; Detector at 90 degree. 2.0 diameter and 3 cm depth of reinforcing bar.

```
c          cell cards
1          1          -2.35  -1 2 -3 4 -5 6 #2   imp:p=1        $  Concrete block
2          2          -7.6    -10 -9 8   imp:p=1               $  Reinforcing bar
3          0          #2 # 1 -11  imp:p=1                      $  Internal void
4          0          11  imp:p=0                              $  External void

c          surface cards
1          px 20.0                $ Plane of concrete block
2          px -20.0               $ Plane of concrete block
3          py 10.0                $ Plane of concrete block
4          py -5.0                $ Plane of concrete block
5          pz 20.0                $ Plane of concrete block
6          pz -20.0               $ Plane of concrete block
7          p -20.0 20.0 0.0 -21.0 19.0 1.0 -21.0 19.0 -1.0      $ Plane of source
8           pz -25.0              $ End of steel bar
9          pz 25.0                $ End of steel bar
10         c/z -7.0 7.0 1.0       $ 2.0 cm. diameter of reinforcing bar
11         so  50                 $ External void

c          data cards
mode p                            $ Photon-only problem
phys:p  .662 1 1                  $ No electron production, no coherent
c          monodirectional disk source
sdef       pos=-20 20 0  dir=1   rad=d1  vec=1 -1 0  axs=1 -1 0
           cel=3 ara=3.1415926535898E+00  erg=0.662  sur=7
si1        1.0                    $ Radius of source
sp1        -21 1                  $ Provided circle, enable uncollided
m1         1001 -1.0E-02  8016 -5.29E-01  6012 -1.0E-03
```

```
          11023 -1.6E-02  12000 -2.0E-03  13027 -3.4E-02
          14000 -3.37E-01  19000 -1.3E-02  20000 -4.4E-      $ Concrete contents
          02  26000 -1.4E-02
m2        26000 1          $ Steel Content
fc5       point detector
f5:p      14.21316448 28.2132424 0 0       $ Position of the detector at 90 degree
e5        0.1 3i 0.225679591 30i 0.313135978 3i 0.662       $ Energy bin for the f5:p detector
nps       300000       $ The simulation will be stopped when 300,000 particles were sampling
print
```

Biography

Mr. Kanpong Choophan was born on March, 17, 1978 in Ayutthaya province. He got Bachelor Degree in Mechanical Engineering from Kasetsart University, Bangkok, Thailand in 1997. Since June 1998, he has been studying in Master Degree in Department of Nuclear Technology, Faculty of Engineering, Chulalongkorn University, Bangkok, Thailand.